TENSILE AND CREEP-RUPTURE BEHAVIOR OF TWO ADVANCED OXIDE DISPERSION STRENGTHENED SHEET ALLOYS

W.H. Wiegert
R.J. Henricks

Pratt and Whitney Aircraft Group,
Commercial Products Division, East Hartford CT

Tensile and creep-rupture properties of Incoloy MA 956 and Haynes Developmental Alloy 8077 have been evaluated and correlated with alloy fracture behavior. An increase in strain rate is associated with an increase in ductility in these alloys. At low strain rates and elevated temperatures MA 956 fails by microvoid formation and coalescence ahead of a moving crack perpendicular to the stress axis with link-up along longitudinal grain boundaries, while HDA 8077 fails in the classical manner of cavitation in transverse oriented grain boundaries leading to intergranular cracking and failure. A critical strain rate which is a function of temperature was determined for MA 956 above which high ductility occurs and below which low ductility occurs. HDA 8077 did not exhibit a well defined critical strain rate, but rather a gradual increase of ductility with strain rate.

INTRODUCTION

High temperature oxide dispersion strengthened (ODS) sheet alloys Incoloy MA 956 and Haynes Development Alloy (HDA) 8077 offer the potential for application in combustor and hot stream components in advanced turbine engines where uncoated oxidation and creep resistance are desired. These materials are currently being evaluated under NASA sponsorship in MATE (Materials for Advanced Turbine Engines) Contract NAS3-20072, Project 3. Whittenberger has investigated the tensile and creep behavior of MA 956 bar (1) and sheet (2) and of several ODS NiCrAl alloys (3). The tensile ductility of MA 956 was shown to decrease with decreasing strain rate, while fracture mode was shown to be a function of strain rate at elevated temperature. The unusual high temperature-low strain rate deformation behavior of MA 956 consisting of localized microvoid formation and coalescence ahead of a moving crack was attributed to the interlocking pancake-grained microstructure preventing the classical inter-

granular failure observed in ODS NiCrAl alloys. The mechanism of this microvoid formation has yet to be determined. The concept of a threshold stress for creep deformation was developed for ODS NiCrAl alloys by Whittenberger (3) and Lin and Sherby (4) and it was realized that negligible strain hardening occurred during creep since cavitation was responsible for the ductility observed in low strain rate creep testing.

A program was conducted with two ODS sheet materials to investigate the tensile and creep-rupture behavior utilizing fractographic and optical metallographic techniques. Incoloy MA 956, a BCC FeCrAl alloy, and HDA 8077, an FCC NiCrAl alloy, both strengthened by a fine dispersion of Y_2O_3, were selected for this investigation. Test temperature, strain rate, ductility and yield strength were correlated with fracture modes leading to an increased understanding of the operative failure mechanisms in these ODS alloys.

EXPERIMENTAL PROCEDURE

Incoloy MA 956 alloy sheet of 1.1-1.3mm (0.043-0.051") thickness was supplied by Wiggin, Ltd. of the International Nickel Company and HDA 8077 alloy sheet of 1.1-1.4mm (0.043-0.055") thickness was supplied by Stellite Division of Cabot corporation. The nominal chemistry of each alloy is shown in Table I. Both sheet materials were produced by mechanical alloying of powder, powder consolidation and a series of hot and/or cold rolling procedures. These processing techniques result in yttria particle sizes on the order of 10^2-10^3Å and in coarse "pancake" grains in the plane of the sheet and elongated grains through the thickness in both alloys (Figures 5A and 5D). Sheet with an as-received mill finish and an anneal of 1177°C (2150°F) for ½ hour in hydrogen was employed throughout the program for tensile and creep-rupture specimen testing.

Tensile testing was conducted from room temperature to 1093°C (2000°F) at a strain rate ($\dot{\varepsilon}$) of $5.0 \times 10^{-3} min^{-1}$ and at room temperature and 982°C (1800°F) at a strain rate of $1.5 \times 10^{1} min^{-1}$; creep-rupture testing was conducted at 982°C (1800°F) and 1093°C (2000°F). To investigate the effect of tensile and creep strain rate on the ductility of these ODS alloys, it became necessary to establish an initial strain rate for the creep tested specimens. This creep strain rate was defined as the quotient of 0.1% strain and the time to reach 0.1% strain.

TABLE 1: NOMINAL CHEMISTRY OF ODS ALLOYS

	Cr	Al	Ti	Y_2O_3	Fe	Ni
Incoloy MA 956	20.0w/o	4.5	0.5	0.5	Bal.	--
HDA 8077	16.0	4.0	--	1.3	--	Bal.

Representative failed tensile and creep specimens were selected for fractographic and optical metallographic examination. To supplement tensile and creep-rupture ductility values (post-test elongations) and gain a measure of localized deformation or necking, the reduction in sheet thickness (RST) for each specimen was calculated from metallographic samples by measuring final thickness as near as possible to the fracture.

RESULTS

Tensile

Tensile results are summarized in Figures 1 and 2. Room temperature tensile testing resulted in ductile transgranular shear failures at both low and high strain rates in the two alloys. At 5.0×10^{-3} Incoloy MA 956 exhibited relatively low elongation (10%) and high reduction in sheet thickness (32%), typical of localized deformation (Figure 1). Fracture microstructures indicate a high degree of necking prior to failure in a shear mode (Figure 3A). HDA 8077 sheet tested under the same conditions had a relatively high elongation (26%) and moderate RST (19%) indicating more uniform deformation than in MA 956 (Figure 1). The fracture microstructure is shown in Figure 4A. Increasing the strain rate to 1.5×10^{1} min^{-1} for the two alloys resulted in more localized deformation as shown by slightly lower overall elongations and greater reductions in sheet thickness and in higher yield strengths (Figure 2).

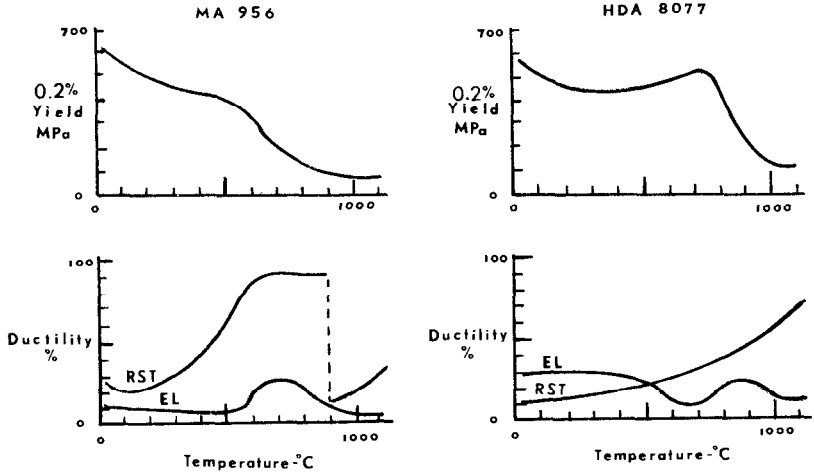

Figure 1. Tensile Properties vs. Temperature Comparison.

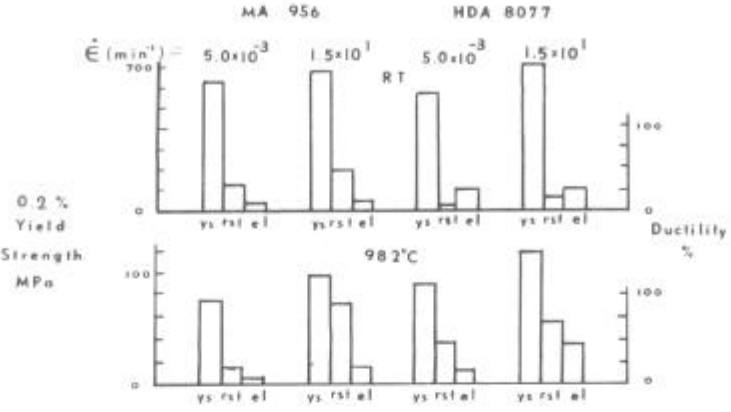

Figure 2. Tensile Properties at Low and High Strain Rates.

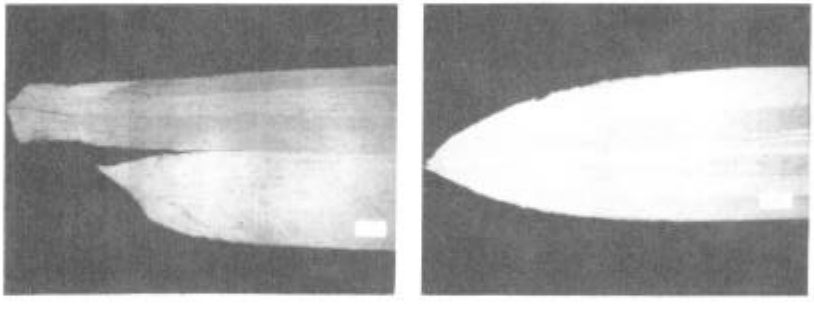

A. RT $\dot{\varepsilon}=5.0\times10^{-3}\,min^{-1}$
0.2%YS=634MPa EL=10% RST=32%

B. 871°C (1600°F) $\dot{\varepsilon}=5.0\times10^{-3}\,min^{-1}$
0.2%YS=150MPa EL=20% RST=89%

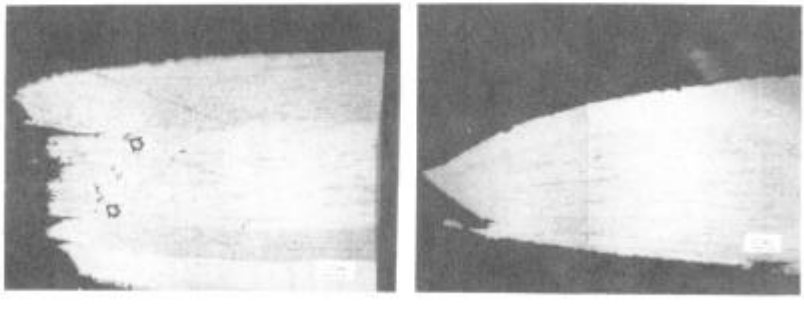

C. 982°C (1800°F) $\dot{\varepsilon}=5.0\times10^{-3}\,min^{-1}$
0.2%YS=94MPa EL=6% RST=17%

D. 982°C (1800°F) $\dot{\varepsilon}=1.5\times10^{1}\,min^{-1}$
0.2%YS=123MPa EL=20% RST=90%

Figure 3. Fracture Microstructures of MA 956 Tensile Tests.

With increasing test temperatures from RT to 1093°C (2000°F) at a constant strain rate of $5.0x10^{-3}min^{-1}$, there is a gradual shift in the operative failure mechanisms in these two alloys. Increasing the test temperature of MA 956 sheet, shifted the fracture mechanisms from ductile shear at room temperature to complete necking at 871°C (1600°F) (Figure 3B) and then to one of microvoid coalescence ahead of a moving crack and transverse grain boundary cavitation at 982°C (1800°F) and above (Figure 3C). This abrupt change in failure mechanism is reflected as a transition in the %RST vs. temperature curve shown in Figure 1. Similarily, the fracture mode of HDA 8077 sheet shifted from planar shear at room temperature to intergranular initiated transgranular failure at 760°C (1400°F) (Figure 4B) and above. Above 871°C (1600°F), the tested HDA 8077 displayed secondary surface cracking and void formation or cavitation on transverse grain boundaries (Figure 4C). A gradual increase in %RST occurs with increased test temperature (Figure 1).

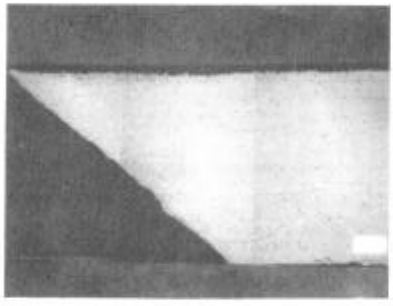

A. RT $\dot{\varepsilon}=5.0x10^{-3}min^{-1}$
0.2%YS=577MPa EL=26% RST=19%

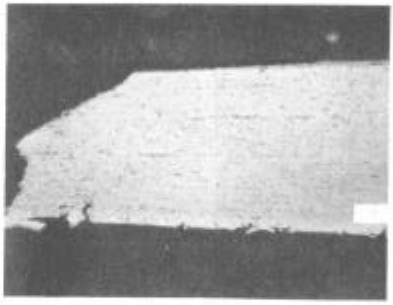

B. 760°C (1400°F) $\dot{\varepsilon}=5.0x10^{-3}min^{-1}$
0.2%YS=556MPa EL=16% RST=43%

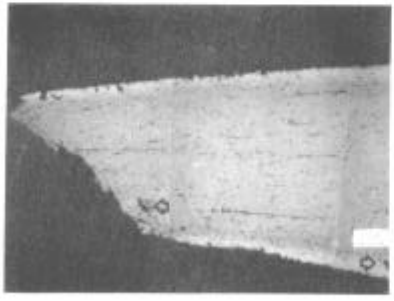

C. 982°C (1800°F) $\dot{\varepsilon}=5.0x10^{-3}min^{-1}$
0.2%YS=165MPa EL=16% RST=44%

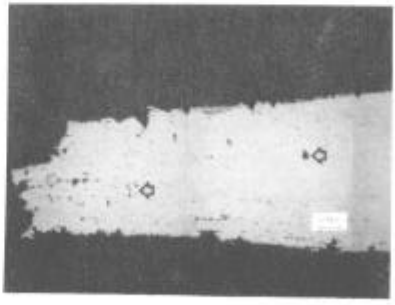

D. 982°C (1800°F) $\dot{\varepsilon}=1.5x10^{1}min^{-1}$
0.2%YS=165MPa EL=47% RST=71%

Figure 4. Fracture Microstructures of HDA 8077 Tensile Tests.

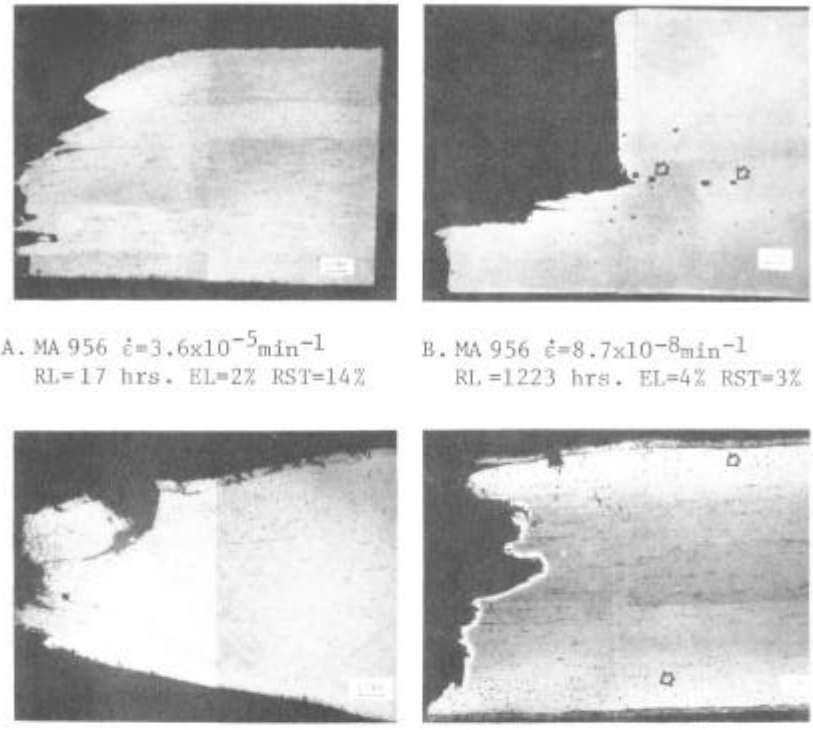

A. MA 956 $\dot{\varepsilon}=3.6\times10^{-5}\text{min}^{-1}$
RL=17 hrs. EL=2% RST=14%

B. MA 956 $\dot{\varepsilon}=8.7\times10^{-8}\text{min}^{-1}$
RL=1223 hrs. EL=4% RST=3%

C. HDA 8077 $\dot{\varepsilon}=1.5\times10^{-4}\text{min}^{-1}$
RL=2 hrs. EL=94% RST=53%

D. HDA 8077 $\dot{\varepsilon}=2.2\times10^{-8}\text{min}^{-1}$
RL=782 hrs. EL=1% RST=5%

Figure 5. Fracture Microstructures of Creep-Rupture Tests.

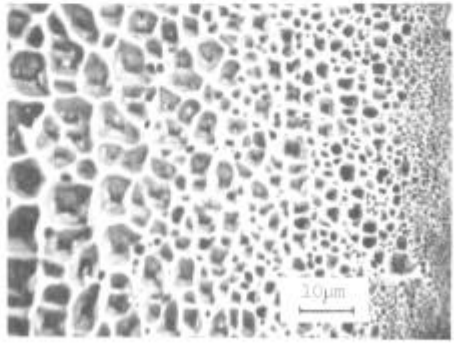

Figure 6. SEM Photograph of Flat Portion of MA 956 Long Time Creep Fracture Test (Figure 5B) Showing Dimpled Appearance of Microvoid Formation and Coalescence Crack Propagation Behavior.

At 982°C (1800°F) increasing the tensile strain rate from $5.0 \times 10^{-3} min^{-1}$ to $1.5 \times 10^{1} min^{-1}$ resulted in greater yield strength, reduction in sheet thickness and elongation in both alloys (Figure 2). No evidence of cavitation on the transverse grain boundaries of MA 956 was observed at the high strain rate (Figure 3D) as was observed at the low strain rate (arrows Figure 3C). A significant increase in internal cracking was observed on the transverse grain boundaries and on stringers of fine grains in HDA 8077 tested at the high strain rate (arrows Figure 4D) compared to the low strain rate tests (Figure 4C).

CREEP-RUPTURE

The creep-rupture behavior of both alloys at 982°C (1800°F) and 1093°C (2000°F) can be catagorized into short time, high strain rate (10^{-5}-$10^{-3} min^{-1}$) tests and long time, low strain rate (10^{-9}-$10^{-5} min^{-1}$) tests using the calculated creep strain rates described in the Experimental Procedure Section. In general, the short time high strain rate creep-rupture tests displayed higher elongations and reductions in sheet thickness than did the long time, low strain rate tests (Figure 5). Fracture microstructures of the short time creep-rupture specimens of either alloy showed little evidence of cavitation at transverse grain boundaries (Figures 5A and 5C) and were similar in that respect to the high strain rate tensile fractures at 982°C (1800°F). However, in the long time creep-rupture fractures (Figures 5B and 5D) different mechanisms were observed. Fracture occurred by transverse crack growth between microvoids in MA 956 and from cavities in transverse grain boundaries and islands of fine grains in HDA 8077 and eventual link-up along longitudinal grain boundaries. The flat transgranular regions in the MA 956 specimen (Figure 5B) displayed a dimpled character due to the formation, coalescence and rupture of microvoids during creep crack growth. A SEM photomicrograph of the dimple character of the flat creep damaged region is shown in Figure 6. The larger matrix voids (arrows Figures 5B and 5D) have been observed in the unstressed condition and are the result of high temperature exposure during creep-rupture testing and are not related to the microvoids formed ahead of a moving crack in MA 956 or at the transverse grain boundaries in either alloy. In long time creep tests MA 956 failed primarily by transgranular crack propagation while HDA 8077 failed principally by intergranular crack growth.

DISCUSSION

Tensile and creep ductility, yield strength and fracture mode of ODS alloys vary with temperature and strain

rate. As the tensile testing temperature is raised from room temperature to 1093°C (2000°F) at a strain rate of $5x10^{-3}$ min^{-1}, both alloys experience a shift in their respective fracture modes which influence strength and ductility. At elevated temperature, these alloys exhibit a weakening of the transverse grain boundaries as evident by the cavitation and subsequent crack propagation at 982°C (1800°F) and above. At this low strain rate, MA 956 shows an increase in localized tensile deformation (%RST) from 260°C (500°F) to 649°C (1200°F) and reaches a plateau at 871°C (1600°F) (Figure 1). A sharp decrease in reduction in sheet thickness occurs at 982°C (1800°F) reflecting the change in fracture mechanism from necking to microvoid coalescence and grain boundary cavitation. HDA 8077 sheet exhibits a gradual increase in localized tensile deformation with increased temperatures at the low strain rate (Figure 1), as the failure character changes from transgranular to intergranular initiated transgranular failure.

An increase in tensile strain rate from $5.0x10^{-3}min^{-1}$ to $1.5x10$ min^{-1} at 982°C (1800°F) results in more ductile behavior in both alloys (Figure 2). Greater yield strength, elongation and reduction in sheet thickness indicate that at high tensile strain rates, the materials are homogenously strain hardening through a greater volume of material than when tested at a lower strain rate. High strain rate testing precludes the occurrence of time-dependent cavitation observed in the low strain rate tested samples.

At elevated temperature and low initial strain rates, creep crack growth in MA 956 occurs by microvoid formation and coalescence leading to link-up along longitudinal grain boundaries. Since deformation only occurs in the region of microvoid formation, little overall elongation or reduction in sheet thickness is observed. Similarily, in HDA 8077, at low strain rates cavitation on transverse grain boundaries leads to transverse transgranular crack growth perpendicular to the stress axis with link-up along the longitudinal grain boundaries. Again the deformation is restricted to regions of cavitation and cracking and results in little elongation or reduction in sheet thickness. Microvoid coalescence crack growth was not observed in HDA 8077 as it was in MA 956 alloy.

High initial strain rate creep testing allows no time for cavitation or slow crack growth; the material necks and strain hardens until the remaining material fails in a ductile manner by tensile overload. This behavior is similar to that of the high strain tensile tested material.

In tensile and creep-rupture testing there is a trade off between temperature and strain rate affecting the

mechanical properties and fracture behavior of ODS alloys; low strain rates lead to generally low ductility behavior while high strain rates lead to high ductility behavior. It is apparent that the efficiency of the dispersion strengthening of these alloys has progressed to the point where, at low strain rates, deformation must occur by microvoid formation, coalescence and crack link-up and growth in MA 956 and by cavitation in HDA 8077. In low strain rate testing it is energetically more favorable to deform in localized areas rather than through a larger volume as in the high strain rate testing. This behavior suggests that there may be critical strain rates for these alloys where fracture modes change significantly. Correlation of tensile and creep-rupture reduction of sheet thickness and strain rate at 982°C (1800°F) superimposed with fracture mechanism in Figure 7 reveals a shift in fracture behavior from one of low ductility to one of high ductility with increasing strain rate.

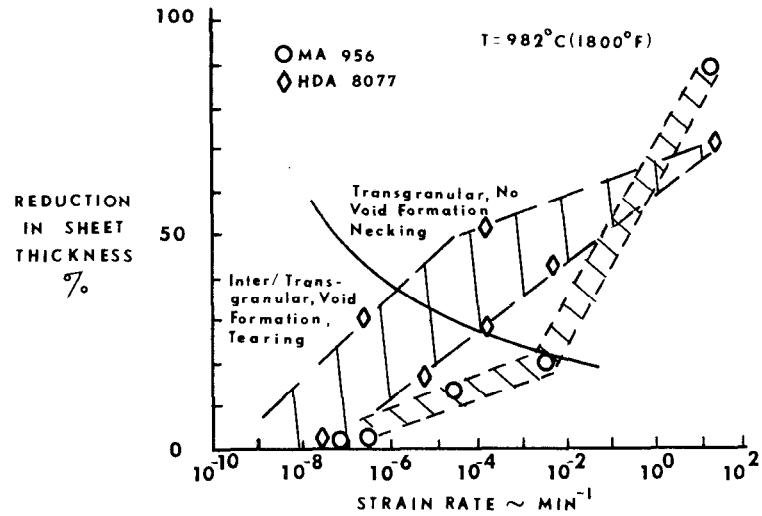

Figure 7. Strain Rate Sensitivity of ODS Alloys

The data shown in Figure 7 suggests that there is a critical strain rate above $5.0x10^{-3}min^{-1}$ for MA 956 at which this fracture mechanism shift occurs; this observation is in agreement with a critical strain rate concept developed by Whittenberger (1) for MA 956 at 1093°C (2000°F). HDA 8077 shows a gradual increase in ductility with no rapid change in behavior as was observed with MA 956.

In addition, examination of Figure 1 reveals a discontinuity in the RST curve for MA 956 indicating that at constant strain rate of $5.0x10^{-3}min^{-1}$ and increasing temperature, there exists a critical temperature at which the one type of fracture character, that of complete necking, becomes one of microvoid coalescence and grain boundary cavitation. This sharp transition in fracture behavior suggests that the critical strain rate is a function of temperature.

CONCLUSIONS

1. Increasing temperature at a constant tensile strain rate ($\dot{\varepsilon}=5.0x10^{-3}min^{-1}$) results in increasing amounts of localized deformation for MA 956 at 20°C (68°F)-760°C (1400°F) and for HDA 8077 at 20°C (68°F)-1093°C (2000°F). MA 956 at 982°C (1800°F) and above exhibits microvoid coalescence and transverse grain boundary cavitation.
2. Increasing tensile strain rate from $5.0x10^{-3}min^{-1}$ to $1.5x10^{1}min^{-1}$ increases the yield strength, elongation and reduction in sheet thickness at 982°C (1800°F) for both alloys. The shorter time, higher strain rate test precluded cavitation which resulted in lower yield strength and ductility at the low strain rate.
3. High temperature, low strain deformation of ODS alloys requires the nucleation and growth of cracks which result in low ductility fracture behavior; as strain rate is increased, there is no time for these materials to crack in this manner and instead they deform through a much larger volume of material resulting in high ductility behavior.
4. Tensile and creep failure modes vary with strain rate, temperature and alloy system. In MA 956 a critical strain rate exists above which high ductility behavior occurs and below which low ductility behavior occurs; this critical strain rate is a function of temperature.

REFERENCES

1. J.D. Whittenberger, Met. Trans. Vol. 10A, 1979, p. 1285-95.
2. J.D. Whittenberger, Met. Trans. Vol. 9A, 1978, p. 101-10.
3. J.D. Whittenberger, Met. Trans. Vol. 8A, 1977, p. 1155-63.
4. J. Lin and O.D. Sherby, NASA CR- 13542, June 1978.